

FLOW AND TURBULENCE NEAR THE EDGE OF A FOREST CANOPY: WIND-TUNNEL AND NUMERICAL EXPERIMENT

Hiroaki Kondo*

National Institute of Advanced Science and Technology (AIST), Tsukuba, JAPAN

Akira Hori

Meteorological & Environmental Sensing Technology Inc., Tsukuba, JAPAN

Ryoko Sakai

Nagoya University, Nagoya, JAPAN

Satoru Iizuka

Nagoya University, Nagoya, JAPAN

Katsuhiko Mutou

AIST, Tsukuba, JAPAN

1. INTRODUCTION

Some flux towers in AsiaFlux sites are located near the top of mountains. Takayama (TKY) in Japan and Sakaerat (SKR) in Thailand are such flux sites, and it is often a problem that the fetch of those sites is not enough for flux measurements. It is not easy to correct the fluxes observed at such site under short-fetch conditions. Computational fluid dynamics, which has rapidly developed in the last two decades, may be a promising method to overcome this problem.

One of the simplest situations describing the short-fetch problem is the analysis of the edge flow and dispersion near the edge of the forest canopy on the contrast of grass land and forest. Park and Paw U (2004) considered dispersion near the edge of the forest canopy with a simple two-dimensional numerical model, in which the profiles of horizontal wind velocity and vertical diffusivity were given as the outer parameters. In their results, the scalar concentration, which was released uniformly inside the canopy, monotonically increased towards downstream as the distance of the inflow edge of the forest canopy increased. A similar situation was calculated with the RANS (Reynolds Averaged Navier-Stokes equation) model and LES (large-eddy simulation) in the present

study. To test the performance of numerical models, a wind-tunnel experiment was employed with a wire-mesh canopy. These trials are in the first stage of the study, and some discrepancies were found among the numerical calculations and the wind-tunnel experiment.

2. NUMERICAL MODELS

Numerical experiments for both RANS and LES were conducted in the domain shown in Fig. 1. The canopy height (H) was set as 18m; the length of the domain was 66.6H, the height, 16.7H, and the width, 11.1H. The canopy was divided into two layers; the leaf area density in the upper half was 0.33, that in the lower half was 0.11, and the LAI was 4. The inflow velocity was vertically uniform, 10 ms⁻¹.

2.1 RANS approach

In the RANS calculation, the standard k-ε model was employed. The basic equations are,

$$\frac{\partial u_i}{\partial t} + \frac{\partial}{\partial x_j} (u_i u_j) = -\frac{1}{\rho_0} \frac{\partial p}{\partial x_i} + \frac{\partial}{\partial x_j} \left\{ \nu_e \left(\frac{\partial u_i}{\partial x_j} + \frac{\partial u_j}{\partial x_i} \right) \right\} - C_d a u_i \sqrt{u_j u_j} \quad (1)$$

*Corresponding author address: Hiroaki Kondo, AIST-west, 16-1, Onogawa Tsukuba, 3058569, JAPAN; e-mail kondo-hrk@aist.go.jp

$$\frac{\partial k}{\partial t} + \frac{\partial}{\partial x_j} (ku_j) = \frac{\partial}{\partial x_j} \left\{ \left(\nu + \frac{\nu_t}{\sigma_k} \right) \frac{\partial k}{\partial x_j} \right\} + (G_s + G_T - \varepsilon) + \underline{C_d a (u_j u_j)^{\frac{3}{2}}} \quad (2)$$

$$\frac{\partial \varepsilon}{\partial t} + \frac{\partial}{\partial x_j} (\varepsilon u_j) = \frac{\partial}{\partial x_j} \left\{ \left(\nu + \frac{\nu_t}{\sigma_\varepsilon} \right) \frac{\partial \varepsilon}{\partial x_j} \right\} + \left\{ C_1 \frac{\varepsilon}{k} (G_s + G_T) - C_2 \frac{\varepsilon^2}{k} \right\} + \frac{\varepsilon}{k} \underline{C_{p\varepsilon} C_d a (u_j u_j)^{\frac{3}{2}}} \quad (3)$$

$$\frac{\partial u_j}{\partial x_j} = 0 \quad (4)$$

where u_i is the wind velocity component, p , the pressure, ν_e , the eddy viscosity, C_d , the effective drag coefficient for leaf, a , the leaf area density. K , the turbulent kinetic energy, ε , the dissipation rate, and G_s , the shear generation. G_T is the buoyancy generation for turbulent kinetic energy, but it is equal to zero in the present neutral case. The underlined parts were additional terms in consideration of the forest canopy (Mochida et al., 2008). The commercial code of α -FLOW was used for the calculation (Kondo et al., 2006).

2.2 LES approach

The standard Smagorinski model was used for the LES calculation (Iizuka and Kondo, 2004). The same domain and boundary condition as those of the RANS model were used for the calculation. The momentum equation with the same additional term as Eq. (1) and the equation of continuity were used; however, the ensemble average was not taken for the LES calculation.

3. RESULTS FROM NUMERICAL MODELS

3.1 Results from the RANS calculation

Figure 2 shows the RANS results for the scalar concentration, which was released from the soil, and the wind vectors. A recirculation appeared around $x=25H$ near the ground in the canopy. The scalar concentration was the highest around the recirculation. Vertical diffusion of the scalar concentration inside the canopy was weak at the upstream side of the recirculation; however, it was strong at the

downstream side. This suggests that the flux from the soil was not measured by the flux tower when the tower was located at the upstream side of the recirculation.

3.2 Comparison with the results from LES

Figure 3 shows a comparison of the recirculation area between RANS and LES. As a whole, the flow pattern was similar; however, the scale of the recirculation was different. The length of the recirculation was twice as large in the LES result as in that of RANS. On the other hand, the starting point of the recirculation was almost the same in both the RANS and LES results.

3.3 Recirculation in the canopy

The dependency of the distance between the canopy edge and the starting point of recirculation in the canopy on LAI has been reported and analyzed by Cassiani et al. (2008). From the scale analysis of the momentum, they obtained the following equation for the distance of the starting point of the recirculation from the canopy edge (L_s):

$$\frac{L_s}{H} = (2\alpha + 1) \frac{P(0)}{U(0)^2} \frac{1}{C_d LAI} \quad ,$$

where $\alpha > 2$. $P(0)$, $U(0)$, and C_d are the pressure difference from that at $x=L_s$, the mean wind velocity at the canopy edge, and the effective drag coefficient for leaf, respectively. Cassiani et al. (2008) considered the forest and clearing of the same length with periodic boundary conditions in the streamwise direction; however, our case involved a long forest canopy without clearing. Even for the case without clearing, recirculation was generated; moreover, L_s was inversely proportional to LAI in our RANS results (not shown).

4. WIND-TUNNEL EXPERIMENT

There were some discrepancies between the results obtained with the RANS and LES models (Fig. 3). To further investigate this, we conducted a wind-tunnel experiment. The fetch of the wind-tunnel experiment was expected to be greater than 45H, as suggested from the results of the numerical experiment, and 50H was employed. Usually, stick-like obstacles or modeled trees are used for this kind of

wind-tunnel experiment (e.g., Moroney, 1968). However, measurements with Laser Doppler Anemometer (LDA) are difficult for a complicated model canopy. Here, we used wire mesh to model the forest canopy. The wind tunnel used here was a thermally stratified wind tunnel in AIST (Kitabayashi, 1991). The scale of the test section was 20m long, 3m wide, and 2m high. A wire mesh that was 2m long and 0.1m high (=H) was equally spaced perpendicularly to the mean wind flow in the wind tunnel at a 0.1m distance. The length of the area in which the wire mesh was set was 5m (=50H, Fig. 4).

4.1 LAI of wire-mesh canopy

Because LAI is a very important parameter for the canopy drag, it should be obtained for the present wire-mesh canopy. The diameter of the wire of the present experiment was 0.0007m, and its pitch was 0.00635m. The effective LAI was obtained from the following equation,

$$-C_d a \langle u_i \rangle \sqrt{\langle u_j \rangle^2} = -\frac{1}{2} C_a \langle u_i \rangle \sqrt{\langle u_j \rangle^2} S$$

The drag coefficient C_a was obtained from the measurement of the drag force of the wire-mesh canopy. Then, the leaf area density a is,

$$a = \frac{1}{2} \frac{C_a}{C_d}$$

From this relation, the effective LAI was estimated to be 0.43.

4.2 Results of the wind-tunnel experiment

Figure 5 shows the variation of the Reynolds stress, TKE, and mean wind velocity at the level of 0.1H along the distance from the edge of the forest canopy. All three variables damped at first due to the barrier effect of the wire-mesh canopy. Then, all the three variables took their minimum; however, the locations were closer to the inflow edge for the second moment. Then, they recovered the values to some extent and maintained nearly constant values. The results of the RANS calculation are shown on the right-hand side of the same figure. The minima of both in the TKE and mean wind velocity are shown; however, those positions were close to each other and further inland from the edge of the canopy than those in the wind-tunnel experiment.

Figure 6 shows the vertical cross section of the

mean wind velocity and TKE along the center line of the canopy. The mean wind velocity took its minimum at $x=17H$ near the bottom of the canopy. TKE was generated at first near the top of the canopy and then extended to both the upper atmosphere and the lower canopy. This figure suggested that the acceleration of the mean wind at the bottom of the canopy comes from the downward transportation of the momentum with the turbulence generated at the top of the canopy. However, further investigation is required.

5. CONCLUSION

The flow and turbulence near the edge of the forest canopy were investigated with the numerical models of RANS and LES and a wind-tunnel experiment. Similar to the cases of Cassiani et al. (2008) with a high LAI, recirculation was generated for the canopy with a LAI of 4, and a length of 66.6H. The starting point of the recirculation was almost the same for the results of both RANS and LES; however, the length of the recirculation was twice as long for RANS as that of LES. The RANS results showed that vertical diffusion was not strong at the upstream side of the recirculation but, rather, at the downstream side. These results suggested that the turbulence character near the edge of the forest canopy was very complicated, similarly to the flow and turbulence around a surface-mounted cube. The wind-tunnel experiment was conducted using a wire-mesh canopy with a LAI=0.43. The main differences between the wind-tunnel experiment and the RANS model are: 1) the minimum of TKE (second moment) appeared closer to the edge than that of the mean flow; however, both minima appeared at nearly the same position in the RANS results. All positions were more towards the interior of the canopy in the RANS results; and 2) TKE was generated near the top of the canopy even from the edge of the canopy in the wind-tunnel experiment; however, the generation of TKE at the top of canopy in the RANS model was very small. Instead, most of TKE was generated inside of the canopy in the RANS results. These characteristics were significantly different from the results with the simple assumption used in the numerical model of Park and Paw U (2004). Further investigation is required to clarify the discrepancy among the RANS, LES, and wind-tunnel results in this area.

6. ACKNOWLEDGEMENT

This study is supported by JSPS Grant-in-Aid for Scientific Research (21241009).

7. REFERENCES

Cassiani, M., G. G. Katul, J. D. Albertson, 2008: The effects of canopy leaf area index on air-flow across forest edges: Large-eddy simulation and analytical results. *Boundary-Layer Meteor.*, 126, 433-460.

Iizuka, S., H. Kondo, 2004: Performance of various sub-grid scale models in large-eddy simulations of turbulent flow over complex terrain. *Atmospheric Environment*, 38, 7083-7091.

Kitabayashi, K., 1991: Wind tunnel simulation of airflow and pollutant diffusion over complex terrain. *Atmospheric Environment*, 25A,

1155-1161.

Kondo, H., K. Asahi, T. Tomizuka, M. Suzuki, 2006: Numerical analysis of diffusion around a suspended expressway by a multi-scale CFD model. *Atmospheric Environment*, 40, 2852-2859.

Meroney, R. N., 1968: Characteristics of wind and turbulence in and above model forest. *J. Appl. Meteor.*, 7, 780-788.

Mochida, A., Y. Tabata, T. Iwata, H. Yoshino, 2008: Examining tree canopy models for CFD prediction of wind environment at pedestrian level. *J. Wind Engineering and Industrial Aerodynamics*, 96, 1667-1677.

Park, Y.-S., K. T. Paw U, 2004: Numerical estimation of horizontal advection inside canopies. *J. Appl. Meteor.*, 43, 1530-1538.

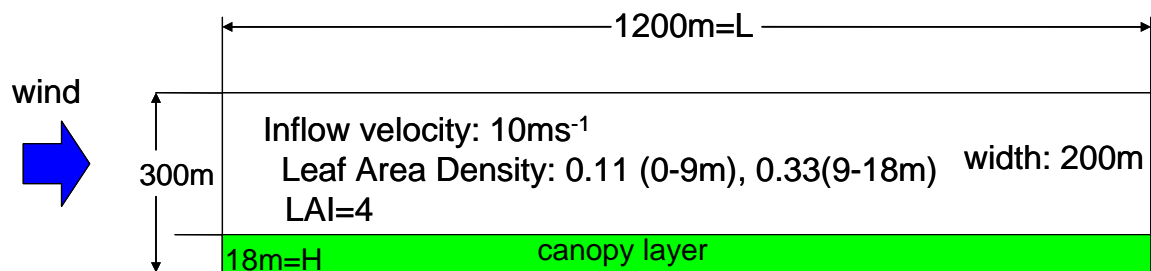


Figure 1 Computational domain for the numerical models.

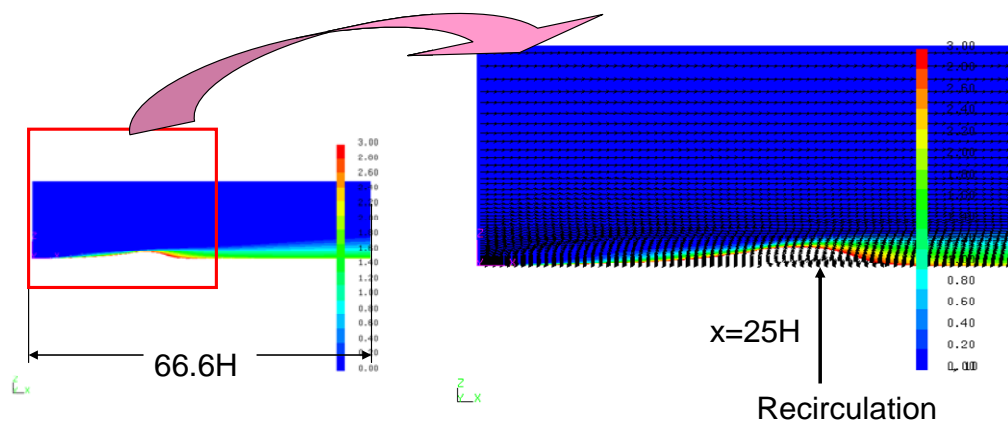


Figure 2 Concentration for uniform surface source and wind vectors from the RANS calculation. Recirculation appeared at $x=25H$, and vertical diffusion was enhanced at the downstream side of the recirculation.

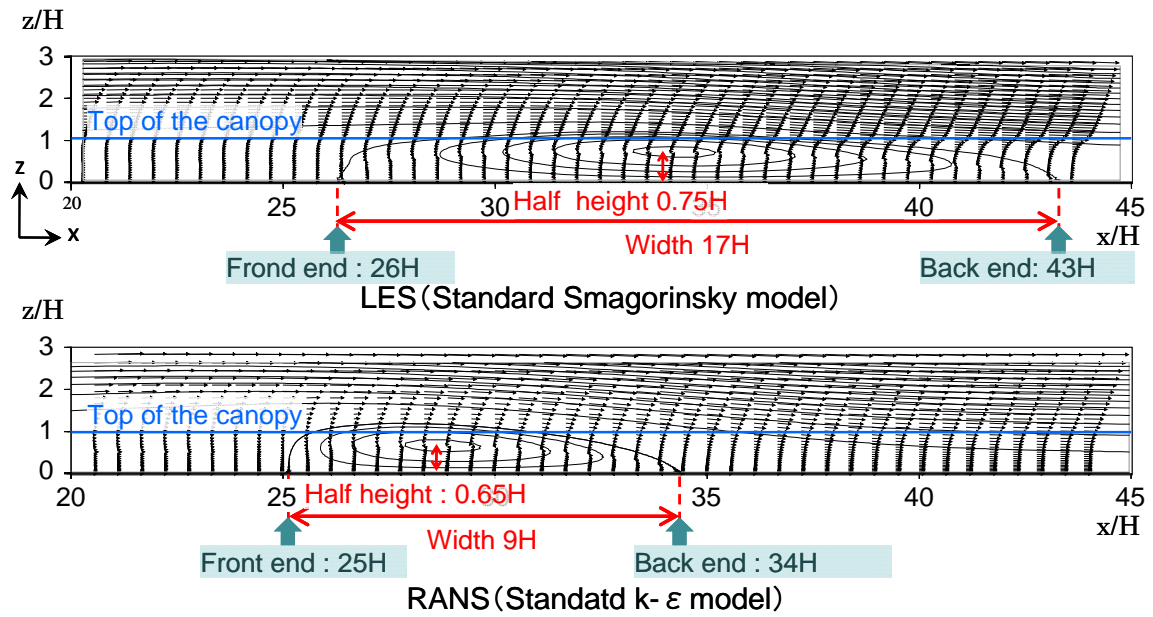


Figure 3 Wind vectors and streamlines near the recirculation for LES result (top) and RANS result (bottom).

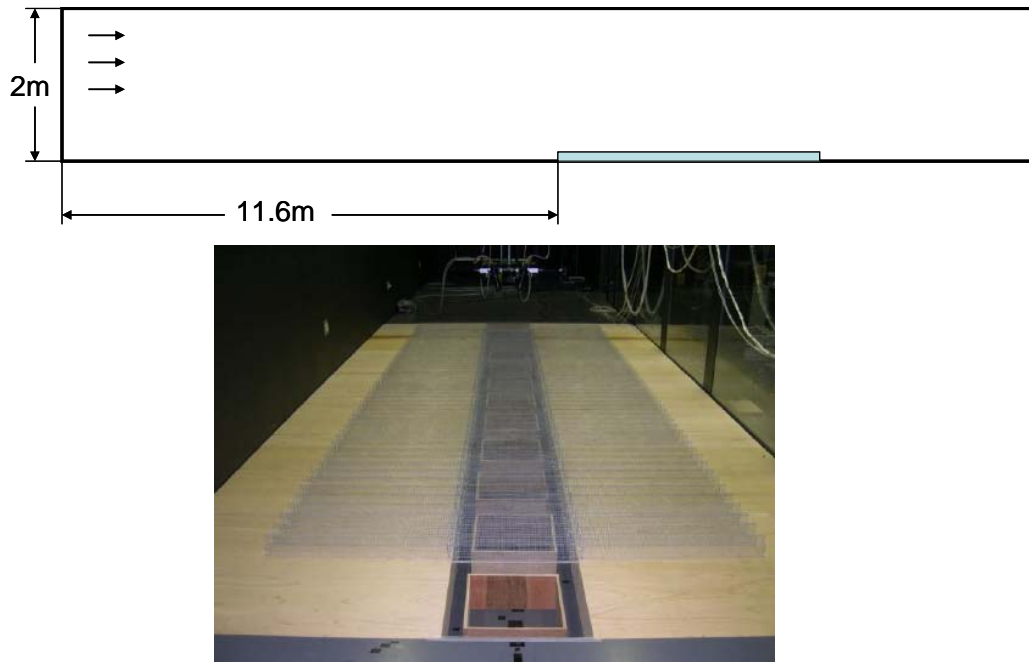


Figure 4 Cross section of the test section in the AIST wind tunnel and location of the wire-mesh canopy (top) and photograph of the wire-mesh canopy in the test section (bottom).

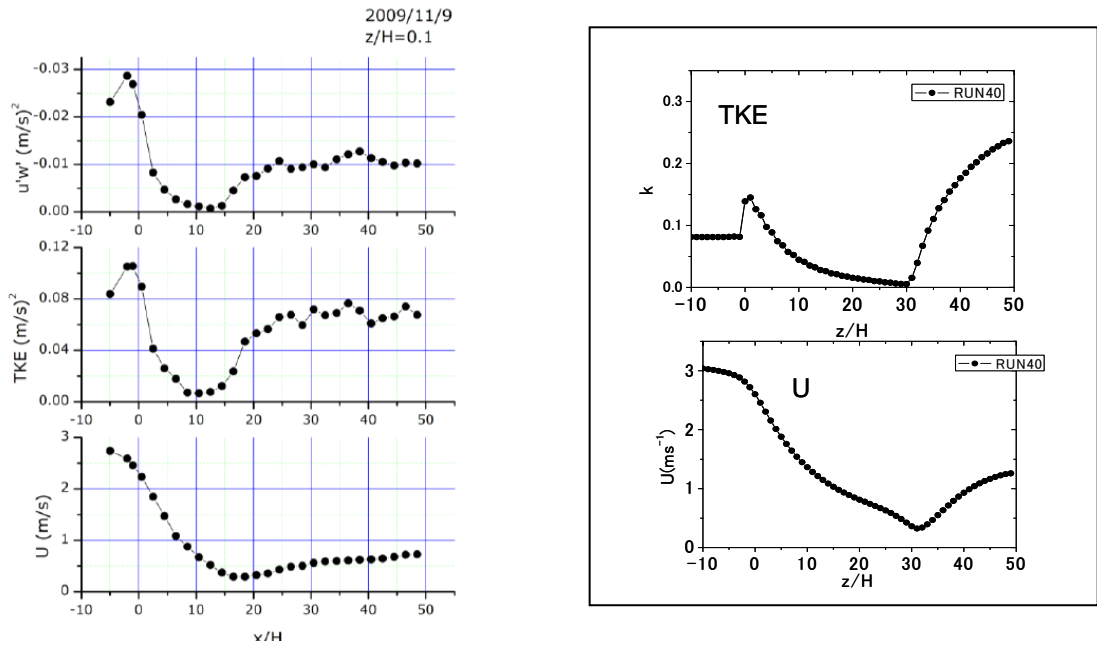


Figure 5 Reynolds stress (top, left), TKE (middle, left), and mean wind velocity at $z=0.1H$ (bottom left) from the wind-tunnel experiment. TKE (right top) and mean wind velocity at $z=0.1H$ (bottom right) from the RANS model.

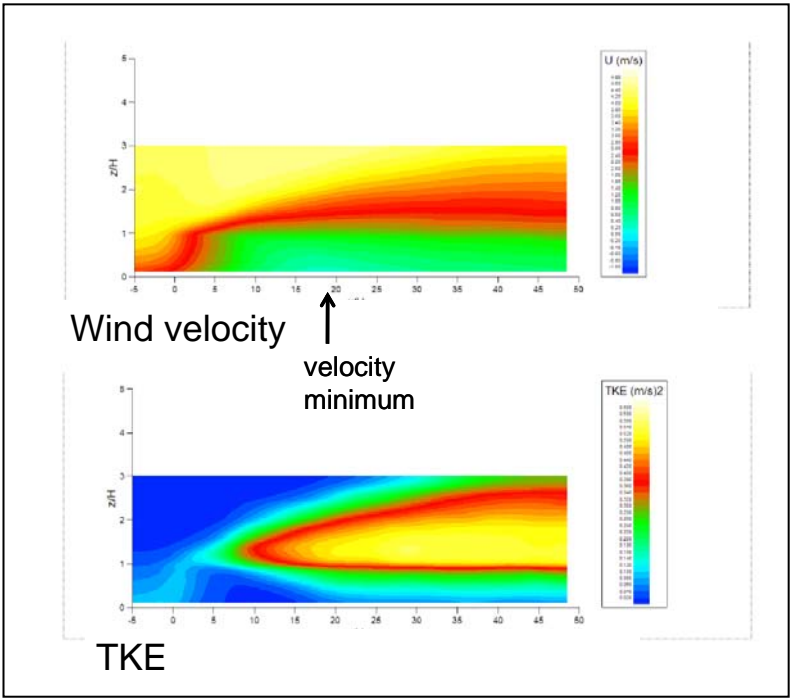


Figure 6 Vertical cross section of the mean wind velocity (top) and TKE (bottom) along the center line of wire-mesh canopy.